Leidenfrost Evaporation-Assisted Ultrasensitive Surface-Enhanced Raman Spectroscopy

Junyeob Song[1, 2], Weifeng Cheng[3], Meitong Nie[2], Xukun He[3], Wonil Nam[2], Jiangtao Cheng[3, *], and Wei Zhou[1, 2 *]

[1]Physical Measurement Laboratory, National Institute of Standards and Technology, Gaithersburg, Maryland 20899, United States
[2]Bradley Department of Electrical & Computer Engineering, Virginia Tech, Blacksburg, Virginia 24061, United States
[3]Department of Mechanical Engineering, Virginia Tech, Blacksburg, Virginia 24061, United States
**Email: chengjt@vt.edu; wzh@vt.edu*

Abstract: Leidenfrost evaporation-assisted Surface-enhanced Raman spectroscopy on hierarchical plasmonic micro/nanostructures provides fast ultrasensitive biochemical detection methods beyond the diffusion limit.

OCIS codes: (250.5403) Plasmonics; (240.6695) Surface-enhanced Raman scattering; (350.4238) Nanophotonics and photonic crystals

1. Summary

Surface-enhanced Raman spectroscopy (SERS) has emerged as an ultrasensitive molecular detection technique for biochemical analyses [1-3]. Due to the significant concentration of light within the sub-nanometer scale near the interface between a metal and dielectric interface, plasmonic nanostructures can achieve a SERS enhancement factor (EF) above 10^7, which is sufficient for single-molecule detection [4-6]. One of the recent efforts in the SERS study is to achieve a fast and ultrasensitive detection of analytes at very low concentrations for applications, including biomedical diagnosis, environmental monitoring, and food safety [7-9]. The diffusion-limited transport process, however, makes it very challenging to accumulate analyte molecules of sub-nanomolar-level concentrations into sub-10-nm hot spots of the SERS substrates within a relatively short detection time window [10]. Recently, we reported a hydrophobic SERS substrate composed of multilayered Au-Ag-Au nanostructures on hierarchical micro-nano pillar arrays, showing high SERS performance with high contact angle profile to enable ultrasensitive SERS detection via breaking the diffusion-limit [11]. Such hydrophobic SERS substrates by integrating nanoplasmonic devices with hierarchical micro-nanopillar structures can be a crucial platform for ultrasensitive bio-/chemical sensing applications.

To reduce the final deposition footprint of analytes by 3-4 orders of magnitude and enable low-concentration SERS measurements of nanomolar analytes in the liquid solution, we demonstrate a SERS measurement strategy with the heat-assisted evaporation technique for hierarchical plasmonic substrates based on Leidenfrost effect. A liquid droplet on a heated surface can be levitated by an insulating vapor layer, which keeps the liquid droplet from boiling rapidly, at the interface between the droplet and the surface [12-13]. Thus, Leidenfrost evaporation of analyte droplets results in a much smaller analyte deposition footprint on hierarchical plasmonic micro/nanostructures, compared to the natural evaporation process, as shown in Figure 1A. It also leads to a much higher analyte molecule density and more intense SERS signals from the detection region. The hierarchical plasmonic structures play important roles in 1) supporting SERS hot spots with high SERS EFs > 10^7 by plasmonic nanostructures, 2) reducing the substrate temperature for Leidenfrost evaporation of liquid droplets, and 3) providing a pinning force at the bottom center of the analyte droplet [14]. We used hierarchical plasmonic micro/nanostructures consisting of Au/Ag nanolaminated plasmonic nanostructures on top of two-tier Si/Carbon-nanotubes (CNT) micro-nanopillar arrays, as shown in Figure 1B. The top-view of the optical image (Figure 1C) shows a dark-color surface, indicating a broadband absorption in the visible spectrum range. The top-view (Figure 1D) and the cross-sectional view (Figure 1E-F) of scanning electron microscopy (SEM) images confirm the microscale uniformity of the hierarchical plasmonic micro/nanostructures.

Besides, the Leidenfrost-assisted evaporation process of droplets in the hybrid Janus state (levitating and pinning) can lead to a much smaller analyte deposition area on hierarchical plasmonic micro/nanostructures, compared to the natural evaporation process (Figure 2A). Leidenfrost evaporation of the R6G droplets in the hybrid Janus state allows direct SERS detection of R6G at a concentration as low as 10^{-9} M, while we cannot observe any R6G Raman signatures through the natural evaporation process. Figure 2B top (bottom) depicts the 2D confocal Raman image at the R6G deposition areas on the hierarchical plasmonic micro/nanostructures with (without) Leidenfrost evaporation, respectively. The spatial distribution patterns of R6G SERS signals at 1508 cm^{-1} are only observed from the Leidenfrost evaporation process, not from the natural evaporation process. This observation confirms that the droplet was in the hybrid Janus state with the final analyte deposition footprint formed both on top of and in the micropillar

cavities of the hierarchical SERS substrate. Figures 2C-D top and bottom show the bright-field images and the fluorescence images of the R6G deposited areas on hierarchical plasmonic micro/nanostructures following Leidenfrost evaporation and natural evaporation, respectively. By Leidenfrost evaporation, the bright-field image (Figure 2C top) clearly shows a red-colored circular-shaped pattern of densely packed R6G molecules with a final R6G deposition area of ~450 μm^2 (deposition size ~ 24 μm), and its shape is in good agreement with the R6G pattern measured by Raman imaging (Figure 2B top) and fluorescence imaging (Figure 2D top) in the same region of the sample. For its reproducibility test, we measured different R6G concentrations ranging from 10^{-5} M to 10^{-9} M with Leidenfrost evaporation, as shown in Figure 2E. In sum, Leidenfrost-assisted SERS on hierarchical plasmonic micro/nanostructures provides a strategy to overcome the diffusion limit for fast and ultrasensitive detection of low-concentration analyte droplets without the need for extra hydrophobic coating on engineered SERS surfaces.

2. Figures

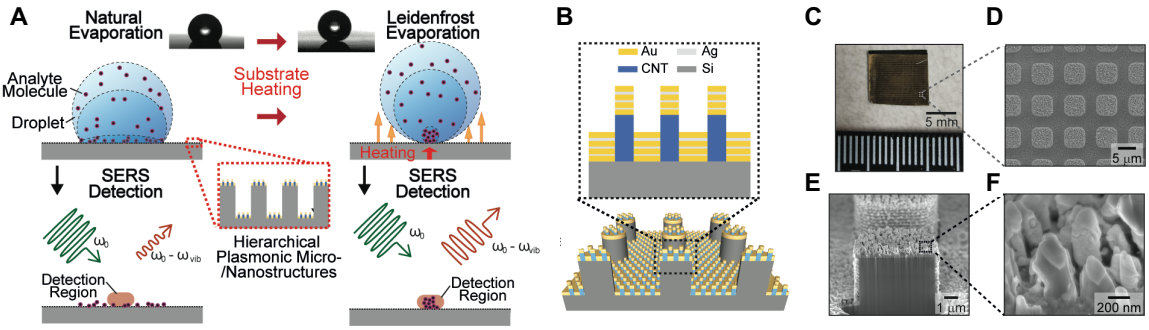

Figure 1. (A) Schematic of Leidenfrost evaporation-assisted SERS detection of analyte molecules in a Janus water droplet on hierarchical plasmonic micro/nanostructures. (B) Schematic illustration of multilayered Au-Ag-Au metal nanostructures on hierarchical micro/nanostructures made of carbon nanopillars and hydrophobic Si micropillars. We deposited alternating layers of Au (25 nm thick) and Ag (6, 8, and 12 nm thick from the bottom to the top) on the two-tier Si/CNT micro/nanopillar array structures (width of 6 um, a micropillar height of 6 um and a periodicity of 9 um) by electron-beam evaporation. (C) Top-view optical image of hierarchical plasmonic micro/nanostructures. (D) Top-view and (E-F) cross-sectional SEM images of hierarchical plasmonic micro/nanostructures.

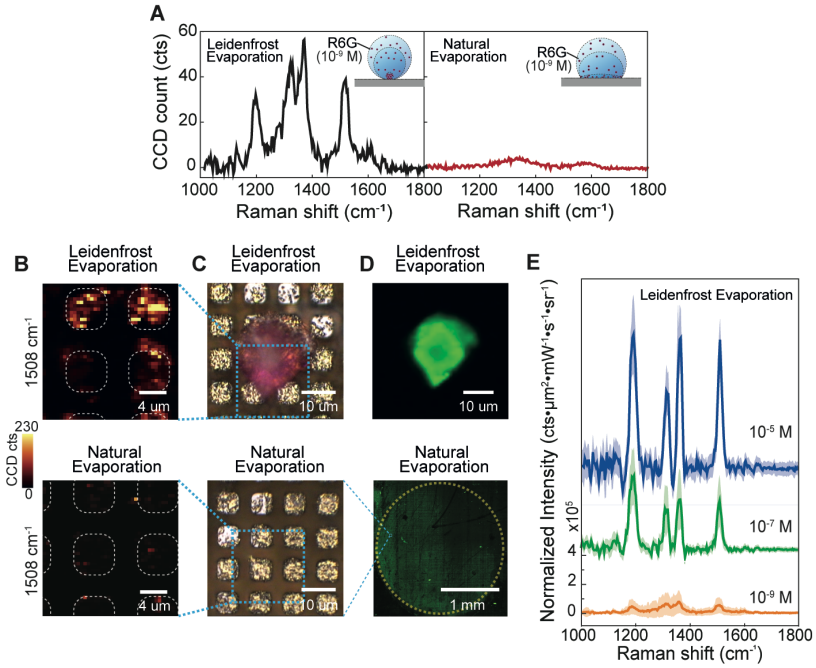

Figure 2. (A) Raman spectra of R6G molecules deposited on hierarchical plasmonic micro/nanostructures via the Leidenfrost evaporation of 20 μL R6G (10^{-9} M) water droplets with substrate heating (left) or natural droplet evaporation without substrate heating (right). (B) confocal Raman images, (C) bright-field images, and (D) fluorescence images of R6G molecules deposited on hierarchical plasmonic micro/nanostructures via the Leidenfrost droplet evaporation with substrate heating (top) or natural droplet evaporation without substrate heating (bottom). (E) Raman spectra with standard deviations (shaded regions) of the deposited R6G molecules via the Leidenfrost evaporation of 20 μL R6G water droplets at different concentrations of 10^{-5} M, 10^{-7} M, and 10^{-9} M (under 785 nm laser excitation and over 20 × 20 pixels at the droplet deposition positions).

3. References

[1] S. S. R. Dasary, A. K. Singh, D. Senapati, H. Yu, and P. C. Ray, “Gold Nanoparticle-Based Label-Free SERS Probe for Ultrasensitive and Selective Detection of Trinitrotoluene,” J. Am. Chem. Soc. **131**, 13806-13812 (2009).

[2] D. A. Stuart, J. M. Yuen, N. Shah, O. Lyandres, C. R. Yonzon, M. R. Glucksberg, J. T. Walsh, and R. P. Van Duyne, “In Vivo Glucose Measurement by Surface-Enhanced Raman Spectroscopy,” Anal. Chem. **78**, 7211-7215 (2006).

[3] J.-F. Li, Y. F. Huang, Y. Ding, Z. L. Yang, S. B. Li, X. S. Zhou, F. R. Fan, W. Zhang, Z. Y.3 Zhou, D. Y. Wu, B. Ren, Z. L. Wang, and Z.-Q. Tian, “Shell-isolated nanoparticle-enhanced Raman spectroscopy,” Nature **464**, 392-395 (2010).

[4] A. Otto, “On the significance of Shalaev’s ‘hot spots’ in ensemble and single-molecule SERS by adsorbates on metallic films at the percolation threshold,” J. Raman Spectrosc. **37**, 937-947 (2006).

[5] J. Song, and W. Zhou, “Multiresonant composite optical nanoantennas by out-of-plane plasmonic engineering,” Nano Lett. **18**, 4409-4416 (2018).

[6] J. Song, W, Nam, and W. Zhou, “Scalable High-Performance Nanolaminated SERS Substrates Based on Multistack Vertically Oriented Plasmonic Nanogaps,” Adv. Mat. Technol. **4**, 1800689 (2019).

[7] R. A. Halvorson and P. J. Vikesland, “Surface-Enhanced Raman Spectroscopy (SERS) for Environmental Analyses,”Environ. Sci. Technol. **44**, 7749-7755 (2010).

[8] A. P. Craig, A. S. Franca, and J. Irudayaraj, “Surface-Enhanced Raman Spectroscopy Applied to Food Safety,” Annu. Rev. Food Sci. Technol. **4**, 369-380 (2013).

[9] C. Zong, M. Xu, L.-J Xu, T. Wei, X. Ma, X.-S. Zheng, R. Hu, and B. Ren, “Surface-Enhanced Raman Spectroscopy for Bioanalysis: Reliability and Challenges,” Chem. Rev. **118**, 4946-4980 (2018).

[10] F. De Angelis, F. Gentile, F. Mecarini, G. Das, M. Moretti, P. Candeloro, M. L. Coluccio, G. Cojoc, A. Accardo, C. Liberale, R. P. Zaccaria, G. Perozziello, L. Tirinato, A. Toma, G. Cuda, R. Cingolani, and E. Di Fabrizio, “Breaking the diffusion limit with super-hydrophobic delivery of molecules to plasmonic nanofocusing SERS structures,” Nat. Photonics **5**, 682 (2011).

[11] J. Song, W. Cheng, J. Cheng, and W. Zhou, "Superhydrophobic SERS Substrates based on Plasmonic Hierarchical Micro-nanostructures," in Frontiers in Optics / Laser Science, OSA Technical Digest (Optical Society of America, 2018), paper JTu3A.82.

[12] H. Kim, B. Truong, J. Buongiorno, and L. W. Hu, “On the effect of surface roughness height, wettability, and nanoporosity on Leidenfrost phenomena,” Appl. Phys. Lett. **98**, 83121 (2011).

[13] L. Zhong and Z. Guo, “Effect of surface topography and wettability on the Leidenfrost effect,” Nanoscale **9**, 6219-6236 (2017).

[14] D. Arnaldo del Cerro., A. G. Marin, G. R. B. E. Römer G, B. Pathiraj, D. Lohse D, and A. J. Huis in’t Veld, “Leidenfrost point reduction on micropatterned metallic surfaces,” Langmuir **28**, 15106-15110 (2012).